Physics Letters B 705 (2011) 193–199

Contents lists available at SciVerse ScienceDirect

Physics Letters B

www.elsevier.com/locate/physletb

High mass exclusive diffractive dijet production in $p\bar{p}$ collisions at $\sqrt{s} = 1.96$ TeV

D0 Collaboration

V.M. Abazov [ai], B. Abbott [bu], M. Abolins [bj], B.S. Acharya [ac], M. Adams [av], T. Adams [at], G.D. Alexeev [ai], G. Alkhazov [am], A. Alton [bi,1], G. Alverson [bh], G.A. Alves [b], L.S. Ancu [ah], M. Aoki [au], Y. Arnoud [n], M. Arov [be], A. Askew [at], B. Åsman [an], O. Atramentov [bm], C. Avila [h], J. BackusMayes [cb], F. Badaud [m], L. Bagby [au], B. Baldin [au], D.V. Bandurin [at], S. Banerjee [ac], E. Barberis [bh], P. Baringer [bc], J. Barreto [b], J.F. Bartlett [au], U. Bassler [r], V. Bazterra [av], S. Beale [f], A. Bean [bc], M. Begalli [c], M. Begel [bs], C. Belanger-Champagne [an], L. Bellantoni [au], S.B. Beri [aa], G. Bernardi [q], R. Bernhard [v], I. Bertram [ao], M. Besançon [r], R. Beuselinck [ap], V.A. Bezzubov [al], P.C. Bhat [au], V. Bhatnagar [aa], G. Blazey [aw], S. Blessing [at], K. Bloom [bl], A. Boehnlein [au], D. Boline [br], T.A. Bolton [bd], E.E. Boos [ak], G. Borissov [ao], T. Bose [bg], A. Brandt [bx], O. Brandt [w], R. Brock [bj], G. Brooijmans [bp], A. Bross [au], D. Brown [q], J. Brown [q], X.B. Bu [g], D. Buchholz [ax], M. Buehler [ca], V. Buescher [x], V. Bunichev [ak], S. Burdin [ao,2], T.H. Burnett [cb], C.P. Buszello [ap], B. Calpas [o], E. Camacho-Pérez [af], M.A. Carrasco-Lizarraga [af], B.C.K. Casey [au], H. Castilla-Valdez [af], S. Chakrabarti [br], D. Chakraborty [aw], K.M. Chan [ba], A. Chandra [bz], G. Chen [bc], S. Chevalier-Théry [r], D.K. Cho [bw], S.W. Cho [ae], S. Choi [ae], B. Choudhary [ab], T. Christoudias [ap], S. Cihangir [au], D. Claes [bl], J. Clutter [bc], M. Cooke [au], W.E. Cooper [au], M. Corcoran [bz], F. Couderc [r], M.-C. Cousinou [o], A. Croc [r], D. Cutts [bw], M. Ćwiok [ad], A. Das [ar], G. Davies [ap], K. De [bx], S.J. de Jong [ah], E. De La Cruz-Burelo [af], F. Déliot [r], M. Demarteau [au], R. Demina [bq], D. Denisov [au], S.P. Denisov [al], S. Desai [au], K. DeVaughan [bl], H.T. Diehl [au], M. Diesburg [au], A. Dominguez [bl], T. Dorland [cb], A. Dubey [ab], L.V. Dudko [ak], D. Duggan [bm], A. Duperrin [o], S. Dutt [aa], A. Dyshkant [aw], M. Eads [bl], D. Edmunds [bj], J. Ellison [as], V.D. Elvira [au], Y. Enari [q], S. Eno [bf], H. Evans [ay], A. Evdokimov [bs], V.N. Evdokimov [al], G. Facini [bh], T. Ferbel [bf,bq], F. Fiedler [x], F. Filthaut [ah], W. Fisher [bj], H.E. Fisk [au], M. Fortner [aw], H. Fox [ao], S. Fuess [au], T. Gadfort [bs], A. Garcia-Bellido [bq], V. Gavrilov [aj], P. Gay [m], W. Geist [s], W. Geng [o,bj], D. Gerbaudo [bn], C.E. Gerber [av], Y. Gershtein [bm], G. Ginther [au,bq], G. Golovanov [ai], A. Goussiou [cb], P.D. Grannis [br], S. Greder [s], H. Greenlee [au], Z.D. Greenwood [be], E.M. Gregores [d], G. Grenier [t], Ph. Gris [m], J.-F. Grivaz [p], A. Grohsjean [r], S. Grünendahl [au], M.W. Grünewald [ad], F. Guo [br], J. Guo [br], G. Gutierrez [au], P. Gutierrez [bu], A. Haas [bp,3], S. Hagopian [at], J. Haley [bh], L. Han [g], K. Harder [aq], A. Harel [bq], J.M. Hauptman [bb], J. Hays [ap], T. Head [aq], T. Hebbeker [u], D. Hedin [aw], H. Hegab [bv], A.P. Heinson [as], U. Heintz [bw], C. Hensel [w], I. Heredia-De La Cruz [af], K. Herner [bi], G. Hesketh [bh], M.D. Hildreth [ba], R. Hirosky [ca], T. Hoang [at], J.D. Hobbs [br], B. Hoeneisen [l], M. Hohlfeld [x], S. Hossain [bu], Z. Hubacek [j], N. Huske [q], V. Hynek [j], I. Iashvili [bo], R. Illingworth [au], A.S. Ito [au], S. Jabeen [bw], M. Jaffré [p], S. Jain [bo], D. Jamin [o], R. Jesik [ap], K. Johns [ar], M. Johnson [au], D. Johnston [bl], A. Jonckheere [au], P. Jonsson [ap], J. Joshi [aa], A. Juste [au,4], K. Kaadze [bd], E. Kajfasz [o], D. Karmanov [ak], P.A. Kasper [au], I. Katsanos [bl], R. Kehoe [by], S. Kermiche [o], N. Khalatyan [au], A. Khanov [bv], A. Kharchilava [bo], Y.N. Kharzheev [ai], D. Khatidze [bw], M.H. Kirby [ax], J.M. Kohli [aa], A.V. Kozelov [al], J. Kraus [bj], A. Kumar [bo], A. Kupco [k], T. Kurča [t], V.A. Kuzmin [ak], J. Kvita [i], S. Lammers [ay], G. Landsberg [bw], P. Lebrun [t], H.S. Lee [ae], S.W. Lee [bb], W.M. Lee [au], J. Lellouch [q], L. Li [as], Q.Z. Li [au], S.M. Lietti [e], J.K. Lim [ae], D. Lincoln [au], J. Linnemann [bj], V.V. Lipaev [al], R. Lipton [au], Y. Liu [g], Z. Liu [f], A. Lobodenko [am], M. Lokajicek [k], P. Love [ao], H.J. Lubatti [cb], R. Luna-Garcia [af,5], A.L. Lyon [au], A.K.A. Maciel [b], D. Mackin [bz], R. Madar [r], R. Magaña-Villalba [af], S. Malik [bl], V.L. Malyshev [ai], Y. Maravin [bd], J. Martínez-Ortega [af], R. McCarthy [br], C.L. McGivern [bc], M.M. Meijer [ah], A. Melnitchouk [bk], D. Menezes [aw], P.G. Mercadante [d], M. Merkin [ak], A. Meyer [u], J. Meyer [w], N.K. Mondal [ac], G.S. Muanza [o], M. Mulhearn [ca],

0370-2693/$ – see front matter
doi:10.1016/j.physletb.2011.10.013

E. Nagy [o], M. Naimuddin [ab], M. Narain [bw], R. Nayyar [ab], H.A. Neal [bi], J.P. Negret [h], P. Neustroev [am], S.F. Novaes [e], T. Nunnemann [y], G. Obrant [am], J. Orduna [af], N. Osman [ap], J. Osta [ba], G.J. Otero y Garzón [a], M. Owen [aq], M. Padilla [as], M. Pangilinan [bw], N. Parashar [az], V. Parihar [bw], S.K. Park [ae], J. Parsons [bp], R. Partridge [bw,3], N. Parua [ay], A. Patwa [bs], B. Penning [au], M. Perfilov [ak], K. Peters [aq], Y. Peters [aq], G. Petrillo [bq], P. Pétroff [p], R. Piegaia [a], J. Piper [bj], M.-A. Pleier [bs], P.L.M. Podesta-Lerma [af,6], V.M. Podstavkov [au], M.-E. Pol [b], P. Polozov [aj], A.V. Popov [al], M. Prewitt [bz], D. Price [ay], S. Protopopescu [bs], J. Qian [bi], A. Quadt [w], B. Quinn [bk], M.S. Rangel [b], K. Ranjan [ab], P.N. Ratoff [ao], I. Razumov [al], P. Renkel [by], P. Rich [aq], M. Rijssenbeek [br], I. Ripp-Baudot [s], F. Rizatdinova [bv], M. Rominsky [au], C. Royon [r], P. Rubinov [au], R. Ruchti [ba], G. Safronov [aj], G. Sajot [n], A. Sánchez-Hernández [af], M.P. Sanders [y], B. Sanghi [au], A.S. Santos [e], G. Savage [au], L. Sawyer [be], T. Scanlon [ap], R.D. Schamberger [br], Y. Scheglov [am], H. Schellman [ax], T. Schliephake [z], S. Schlobohm [cb], C. Schwanenberger [aq], R. Schwienhorst [bj], J. Sekaric [bc], H. Severini [bu], E. Shabalina [w], V. Shary [r], A.A. Shchukin [al], R.K. Shivpuri [ab], V. Simak [j], V. Sirotenko [au], P. Skubic [bu], P. Slattery [bq], D. Smirnov [ba], K.J. Smith [bo], G.R. Snow [bl], J. Snow [bt], S. Snyder [bs], S. Söldner-Rembold [aq], L. Sonnenschein [u], A. Sopczak [ao], M. Sosebee [bx], K. Soustruznik [i], B. Spurlock [bx], J. Stark [n], V. Stolin [aj], D.A. Stoyanova [al], E. Strauss [br], M. Strauss [bu], D. Strom [av], L. Stutte [au], P. Svoisky [bu], M. Takahashi [aq], A. Tanasijczuk [a], W. Taylor [f], M. Titov [r], V.V. Tokmenin [ai], D. Tsybychev [br], B. Tuchming [r], C. Tully [bn], P.M. Tuts [bp], L. Uvarov [am], S. Uvarov [am], S. Uzunyan [aw], R. Van Kooten [ay], W.M. van Leeuwen [ag], N. Varelas [av], E.W. Varnes [ar], I.A. Vasilyev [al], P. Verdier [t], L.S. Vertogradov [ai], M. Verzocchi [au], M. Vesterinen [aq], D. Vilanova [r], P. Vint [ap], P. Vokac [j], H.D. Wahl [at], M.H.L.S. Wang [bq], J. Warchol [ba], G. Watts [cb], M. Wayne [ba], M. Weber [au,7], L. Welty-Rieger [ax], M. Wetstein [bf], A. White [bx], D. Wicke [x], M.R.J. Williams [ao], G.W. Wilson [bc], S.J. Wimpenny [as], M. Wobisch [be], D.R. Wood [bh], T.R. Wyatt [aq], Y. Xie [au], C. Xu [bi], S. Yacoob [ax], R. Yamada [au], W.-C. Yang [aq], T. Yasuda [au], Y.A. Yatsunenko [ai], Z. Ye [au], H. Yin [g], K. Yip [bs], H.D. Yoo [bw], S.W. Youn [au], J. Yu [bx], S. Zelitch [ca], T. Zhao [cb], B. Zhou [bi], J. Zhu [bi], M. Zielinski [bq], D. Zieminska [ay], L. Zivkovic [bp]

[a] *Universidad de Buenos Aires, Buenos Aires, Argentina*
[b] *LAFEX, Centro Brasileiro de Pesquisas Físicas, Rio de Janeiro, Brazil*
[c] *Universidade do Estado do Rio de Janeiro, Rio de Janeiro, Brazil*
[d] *Universidade Federal do ABC, Santo André, Brazil*
[e] *Instituto de Física Teórica, Universidade Estadual Paulista, São Paulo, Brazil*
[f] *Simon Fraser University, Vancouver, British Columbia, and York University, Toronto, Ontario, Canada*
[g] *University of Science and Technology of China, Hefei, People's Republic of China*
[h] *Universidad de los Andes, Bogotá, Colombia*
[i] *Charles University, Faculty of Mathematics and Physics, Center for Particle Physics, Prague, Czech Republic*
[j] *Czech Technical University in Prague, Prague, Czech Republic*
[k] *Center for Particle Physics, Institute of Physics, Academy of Sciences of the Czech Republic, Prague, Czech Republic*
[l] *Universidad San Francisco de Quito, Quito, Ecuador*
[m] *LPC, Université Blaise Pascal, CNRS/IN2P3, Clermont, France*
[n] *LPSC, Université Joseph Fourier Grenoble 1, CNRS/IN2P3, Institut National Polytechnique de Grenoble, Grenoble, France*
[o] *CPPM, Aix-Marseille Université, CNRS/IN2P3, Marseille, France*
[p] *LAL, Université Paris-Sud, CNRS/IN2P3, Orsay, France*
[q] *LPNHE, Universités Paris VI and VII, CNRS/IN2P3, Paris, France*
[r] *CEA, Irfu, SPP, Saclay, France*
[s] *IPHC, Université de Strasbourg, CNRS/IN2P3, Strasbourg, France*
[t] *IPNL, Université Lyon 1, CNRS/IN2P3, Villeurbanne, France and Université de Lyon, Lyon, France*
[u] *III. Physikalisches Institut A, RWTH Aachen University, Aachen, Germany*
[v] *Physikalisches Institut, Universität Freiburg, Freiburg, Germany*
[w] *II. Physikalisches Institut, Georg-August-Universität Göttingen, Göttingen, Germany*
[x] *Institut für Physik, Universität Mainz, Mainz, Germany*
[y] *Ludwig-Maximilians-Universität München, München, Germany*
[z] *Fachbereich Physik, Bergische Universität Wuppertal, Wuppertal, Germany*
[aa] *Panjab University, Chandigarh, India*
[ab] *Delhi University, Delhi, India*
[ac] *Tata Institute of Fundamental Research, Mumbai, India*
[ad] *University College Dublin, Dublin, Ireland*
[ae] *Korea Detector Laboratory, Korea University, Seoul, Republic of Korea*
[af] *CINVESTAV, Mexico City, Mexico*
[ag] *FOM-Institute NIKHEF and University of Amsterdam/NIKHEF, Amsterdam, The Netherlands*
[ah] *Radboud University Nijmegen/NIKHEF, Nijmegen, The Netherlands*
[ai] *Joint Institute for Nuclear Research, Dubna, Russia*
[aj] *Institute for Theoretical and Experimental Physics, Moscow, Russia*
[ak] *Moscow State University, Moscow, Russia*
[al] *Institute for High Energy Physics, Protvino, Russia*
[am] *Petersburg Nuclear Physics Institute, St. Petersburg, Russia*
[an] *Stockholm University, Stockholm and Uppsala University, Uppsala, Sweden*
[ao] *Lancaster University, Lancaster LA1 4YB, United Kingdom*
[ap] *Imperial College London, London SW7 2AZ, United Kingdom*

[aq] The University of Manchester, Manchester M13 9PL, United Kingdom
[ar] University of Arizona, Tucson, AZ 85721, USA
[as] University of California Riverside, Riverside, CA 92521, USA
[at] Florida State University, Tallahassee, FL 32306, USA
[au] Fermi National Accelerator Laboratory, Batavia, IL 60510, USA
[av] University of Illinois at Chicago, Chicago, IL 60607, USA
[aw] Northern Illinois University, DeKalb, IL 60115, USA
[ax] Northwestern University, Evanston, IL 60208, USA
[ay] Indiana University, Bloomington, IN 47405, USA
[az] Purdue University Calumet, Hammond, IN 46323, USA
[ba] University of Notre Dame, Notre Dame, IN 46556, USA
[bb] Iowa State University, Ames, IA 50011, USA
[bc] University of Kansas, Lawrence, KS 66045, USA
[bd] Kansas State University, Manhattan, KS 66506, USA
[be] Louisiana Tech University, Ruston, LA 71272, USA
[bf] University of Maryland, College Park, MD 20742, USA
[bg] Boston University, Boston, MA 02215, USA
[bh] Northeastern University, Boston, MA 02115, USA
[bi] University of Michigan, Ann Arbor, MI 48109, USA
[bj] Michigan State University, East Lansing, MI 48824, USA
[bk] University of Mississippi, University, MS 38677, USA
[bl] University of Nebraska, Lincoln, NE 68588, USA
[bm] Rutgers University, Piscataway, NJ 08855, USA
[bn] Princeton University, Princeton, NJ 08544, USA
[bo] State University of New York, Buffalo, NY 14260, USA
[bp] Columbia University, New York, NY 10027, USA
[bq] University of Rochester, Rochester, NY 14627, USA
[br] State University of New York, Stony Brook, NY 11794, USA
[bs] Brookhaven National Laboratory, Upton, NY 11973, USA
[bt] Langston University, Langston, OK 73050, USA
[bu] University of Oklahoma, Norman, OK 73019, USA
[bv] Oklahoma State University, Stillwater, OK 74078, USA
[bw] Brown University, Providence, RI 02912, USA
[bx] University of Texas, Arlington, TX 76019, USA
[by] Southern Methodist University, Dallas, TX 75275, USA
[bz] Rice University, Houston, TX 77005, USA
[ca] University of Virginia, Charlottesville, VA 22901, USA
[cb] University of Washington, Seattle, WA 98195, USA

ARTICLE INFO

Article history:
Received 13 September 2010
Received in revised form 5 October 2011
Accepted 6 October 2011
Available online 12 October 2011
Editor: M. Doser

ABSTRACT

We present evidence for diffractive exclusive dijet production with an invariant dijet mass greater than 100 GeV in data collected with the D0 experiment at the Fermilab Tevatron Collider. A discriminant based on calorimeter information is used to measure a significant number of events with little energy (typically less than 10 GeV) outside the dijet system, consistent with the diffractive exclusive dijet production topology. The probability for these events to be explained by other dijet production processes is 2×10^{-6}, corresponding to a 4.7 standard deviation significance.

Hard diffraction was first observed about twenty years ago in the UA8 experiment at the CERN $p\bar{p}$ collider SPS [1] and has been studied extensively in several experiments: H1 and ZEUS at the DESY ep Collider HERA [2] and D0 and CDF at the Fermilab Tevatron [3]. At hadron colliders, hard diffractive events are identified by the signature of a high transverse momentum interaction in the presence of a region devoid of any activity in the forward region of the detector or by tagging beam hadrons in the final state. Hard diffractive events can be described by the exchange of a colorless object (Pomeron) [4]. Diffractively produced objects such as dijets, diphotons and χ_c charmonium can be observed in the detector together with Pomeron remnants. A subset of hard diffractive events in which both incoming hadrons remain intact is defined in such a way that the energy not carried away by the outgoing beam particles is used to produce the diffractive system [5,6]. This mechanism is defined as hard exclusive diffractive production (EDP). We search for this production mechanism in a sample of dijet events with large dijet invariant mass, corresponding to large values of the reduced center-of-mass energy of the Pomeron system.

Exclusive diffractive production of a final state X, $p\bar{p} \to p + X + \bar{p}$, has been proposed as a search channel for new physics, as well as for the Higgs boson, at the Large Hadron Collider (LHC) [7]. In this process, the kinematic properties such as the mass of the object X can be computed with high precision by measuring only the momentum loss of the outgoing protons in the final state. The CDF Collaboration reported the observation of exclusive diffractive events in the dijet, dielectron, diphoton and charmonium channels [8]. These results support the existence of EDP, but are restricted to low mass objects (typically less than 100 GeV), while at the LHC, searches for new physics are expected to extend to higher masses. In this Letter, we report evidence for exclusive diffractive

[1] Augustana College, Sioux Falls, SD, USA.
[2] The University of Liverpool, Liverpool, UK.
[3] SLAC, Menlo Park, CA, USA.
[4] ICREA/IFAE, Barcelona, Spain.
[5] Centro de Investigacion en Computacion – IPN, Mexico City, Mexico.
[6] ECFM, Universidad Autonoma de Sinaloa, Culiacán, Mexico.
[7] Universität Bern, Bern, Switzerland.

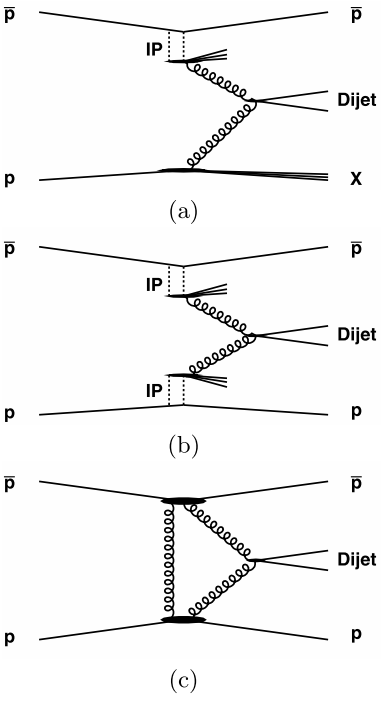

Fig. 1. Production of central dijet events in hard diffraction: (a) single diffraction, in which only either the proton or the antiproton is diffracted by a Pomeron ($\mathbb{P}$) exchange, while the other breaks up; (b) inclusive double Pomeron production, where proton and antiproton remain intact, and additional QCD radiation can be observed from Pomeron remnants; and (c) exclusive diffractive production where both protons remain intact and only the dijet system is produced in the central region.

dijet production with invariant masses greater than 100 GeV in data collected by the D0 experiment.

We consider three different classes of hard diffractive production in addition to non-diffractive production: single diffractive (SD) dijet production (Fig. 1(a)), inclusive diffractive production through double Pomeron exchange (IDP) (Fig. 1(b)), and exclusive diffractive dijet production (Fig. 1(c)). In SD, one of the beam hadrons remains intact while the other breaks up. In IDP, both beam hadrons are intact after the collision. The IDP and EDP processes with proton dissociations are expected to be suppressed by about a factor ten relative to the channel where the beam hadrons remain intact [9]. The parton distributions of the Pomeron are taken from recent H1 measurements [10] and are used to compute the diffractive jet production cross section at the Tevatron. An additional multiplicative factor (gap survival probability) [11] of 0.1 is introduced to account for soft production of particles from the underlying $p\bar{p}$ events that populate the rapidity gaps of the diffractive events [4].

The background to EDP in the dijet mass region considered here originates from SD, IDP and non-diffractive (NDF) events which have either low multiplicity or small energy deposits in the forward calorimeters. Due to the steeply falling nature of these distributions, backgrounds are expected to be small. NDF background events are generated using the PYTHIA v6.202 [12] Monte Carlo (MC) generator with default settings and the diffractive (SD and IDP) backgrounds are determined using the POMWIG v2.0 [13] and FPMC v1.0 [9] generators, respectively. EDP events are generated at the lowest order of QCD through the exchange of two gluons [6] using FPMC.

The data used in this analysis were collected with the D0 detector in the period between August 2002 and April 2006 at the Tevatron Collider at a center-of-mass energy $\sqrt{s} = 1.96$ TeV. The D0 detector is described in detail elsewhere [14]. For this analysis, the most relevant components are the central and forward calorimeters used for jet reconstruction and the identification of a rapidity gap devoid of any energy (above noise) in the calorimeter, respectively. The D0 liquid argon and uranium calorimeter is divided into three parts housed in independent cryostats covering the following regions in pseudo-rapidity: $|\eta| < 1.1$ (central calorimeter), and $1.6 < |\eta| < 4.2$ (two forward calorimeters), where $\eta = -\ln[\tan(\theta/2)]$ and θ is the polar angle with respect to the beam axis. Jets in EDP events are expected to be more central than in the other jet production processes, therefore both jets are required to be central with a rapidity $|y| < 0.8$, where the rapidity is defined as $y = 0.5\ln(E + p_z)/(E - p_z)$ and E is the jet energy and p_z the momentum component of the jet along the beam axis. The forward region of the calorimeter is used to check for the presence of a rapidity gap on each side of the dijet system.

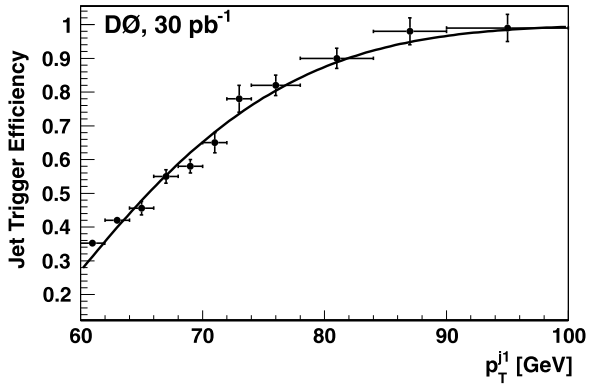

Fig. 2. Jet trigger efficiency as a function of the leading jet p_T (p_T^{j1}). For events with $p_T^{j1} > 100$ GeV, the efficiency is close to 100% and no correction is needed.

The instantaneous luminosity used in this analysis is required to be in the range $[5\text{–}100] \times 10^{30}$ cm^{-2} s^{-1}, where the contribution from two or more $p\bar{p}$ interactions in a single event is in general much less than 20%. This reduces the contamination of multiple interactions in the same bunch crossing to the rapidity gap selection. Data were collected using an inclusive jet trigger requiring at least one jet in an event to be above a p_T threshold of 45 GeV on the uncorrected energy, in order to select exclusive diffractive events in the region of dijet invariant mass above 100 GeV. Due to prescales imposed to avoid saturating the data acquisition system rate capabilities, the equivalent integrated luminosity of the sample is about 30 pb^{-1}. By comparing the highest-p_T jet spectrum with data collected with a trigger with a lower p_T threshold of 15 GeV, the trigger was found not to be fully efficient for jet p_T between 60 and 100 GeV and the Monte Carlo events were reweighted with the trigger efficiency in this jet p_T range. The trigger efficiency as a function of jet p_T is shown in Fig. 2.

Jets are reconstructed using an iterative midpoint cone algorithm [15] with a cone size $\mathcal{R} = \sqrt{(\Delta\eta)^2 + (\Delta\varphi)^2} = 0.7$, where φ is the azimuthal angle. The highest-p_T and second-highest p_T jets are required to be greater than 60 and 40 GeV, respectively, and only dijet events with an invariant mass less than 160 GeV are used in the final analysis. To enhance the number of events without additional QCD radiation [6], the two jets are required to be back-to-back in azimuthal angle φ, with a separation $\Delta\varphi > 3.1$. A possible contribution of fake dijet events due to cosmic rays is suppressed by the requirement that the missing transverse momentum is less than 70% of the leading jet transverse momentum.

The MC events are required to satisfy the same selection criteria as the data. They are processed through a GEANT-based [16] simulation of the D0 detector response and the same reconstruction code as data. To simulate calorimeter noise and the effects of ad-

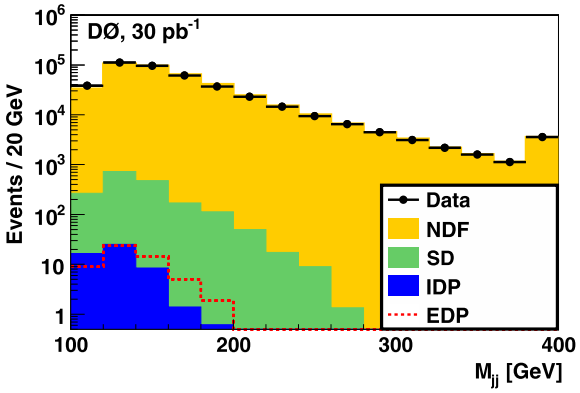

Fig. 3. Dijet invariant mass distribution for MC and data. The last bin contains all events with $M_{jj} > 380$ GeV. Good agreement between the MC simulation and data is found after applying jet energy scale corrections and scale factors corresponding to the trigger efficiencies, the luminosity profiles, and the MC normalization.

ditional $p\bar{p}$ interactions, data events from random $p\bar{p}$ crossings are overlaid on the MC events, using data from the same time period as considered in the analysis. The MC events are weighted to obtain the same instantaneous luminosity profile as the data to have the same additional energy deposits in the forward region of the calorimeter as in data. The sum of the number of NDF, SD, and IDP events is normalized to data after all selection cuts, including the cut on the dijet invariant mass. The contributions from each sample are determined from theoretical cross sections with selection efficiencies applied.[8] The EDP contribution is expected to be negligible at this stage. In Fig. 3, good agreement between the MC simulation and data is seen in the dijet invariant mass (M_{jj}) distribution before the cut on M_{jj}. By varying the requirement on the leading jet p_T, the uncertainty on the normalization was estimated to be 5%.

To discriminate between exclusive events and background (NDF, SD and IDP), we exploit the large rapidity gap that is expected between the central jets and the proton and antiproton beams. Two separate regions of pseudorapidity η are defined in the calorimeter far from the two central jets. The very forward region ($3.0 < |\eta| < 4.2$) allows discrimination of diffractive events (SD and IDP) from NDF events, which are accompanied by beam remnants in this region of the calorimeter. The intermediate forward region ($2.0 < |\eta| < 3.0$) is used to identify EDP events, since they show larger rapidity gaps than SD and IDP. To prevent contamination by noise in the calorimeter region under consideration, noisy cells in the forward region of the calorimeters, which display an occupancy that differs by more than five standard deviations from the average, are removed. The cell response in MC was also adjusted to data by applying a MC-to-data correction factor for each cell. This correction factor was obtained using data collected requiring either minimal activity in the D0 luminosity counters or the presence of low p_T jets. After performing these corrections, the calorimeter cell information is used to form the variable:

$$\Delta = \frac{1}{2}\exp\Big(-\sum_{2<|\eta|<3} E_T\Big) + \frac{1}{2}\exp\Big(-\sum_{3<|\eta|<4.2} E_T\Big) \qquad (1)$$

in order to discriminate between the different classes of events. Here, E_T is the transverse energy in a given cell, and the sum is performed over all cells in the indicated rapidity range. Fig. 4 displays the Δ distribution normalized to unity for all MC samples.

[8] The total selection efficiencies for NDF, SD, IDP and EDP samples are $\approx 0.1\%$, $\approx 0.5\%$, $\approx 1.2\%$ and $\approx 1.7\%$, respectively. For the NDF sample only events with $M_{jj} > 80$ GeV at the parton level are considered in the efficiency calculation.

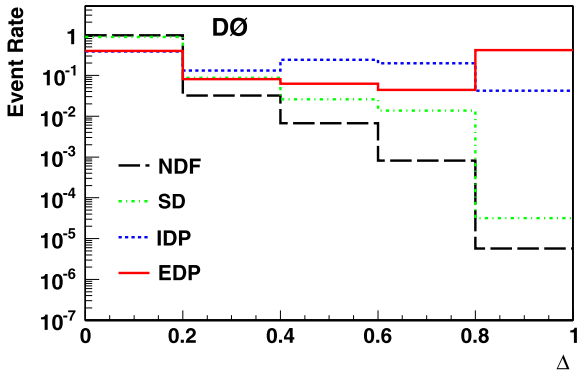

Fig. 4. Distribution of Δ normalized to unity for the MC samples. EDP peaks at $\Delta > 0.8$. The EDP contribution at low Δ values is due to pile-up events, where a second proton–antiproton inelastic scattering occurs in the same bunch crossing.

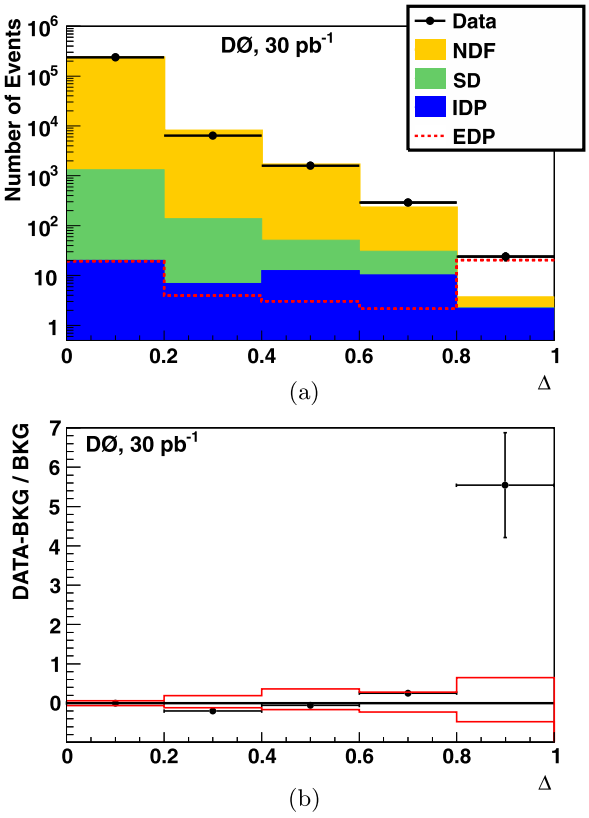

Fig. 5. (a) Distribution of Δ for data and stacked background (NDF, SD and IDP). (b) Normalized difference between data and NDF, SD and IDP processes. The red solid lines are ± 1 standard deviation systematic uncertainties on the background. (For interpretation of the references to color in this figure, the reader is referred to the web version of this Letter.)

Also shown is the expected distribution of EDP events, showing a characteristic peak at $\Delta > 0.8$, corresponding to energy deposits in the forward calorimeter which are typically smaller than 10 GeV.

Systematic uncertainties are assessed on the MC background prediction of the differential Δ distribution. The leading systematic uncertainty is due to the calorimeter cell calibration factors. They are varied simultaneously by three standard deviations from their central value leading to a change of 25% of the background for $\Delta > 0.8$. The effect of the jet energy scale uncertainties modifies the background by 12%. The jet energy resolution in simulation has been varied to match the data, yielding a small change of the normalization of 0.5% which is assigned as an uncertainty. To esti-

mate the uncertainties of the trigger efficiency correction and the instantaneous luminosity reweighting, the analysis was repeated using a 15 GeV jet p_T trigger threshold resulting in a 3% systematic shift. An additional systematic uncertainty due to normalizing the sum of MC events to data is estimated to be 5%. An uncertainty of 50% on the SD and IDP MC cross sections accounts for the uncertainty on the partonic structure of the Pomeron and gap survival probability factor. The non-diffractive parton distribution function uncertainties were considered and found to be negligible compared to the other uncertainties. The total background prediction is $3.7^{+2.4}_{-1.7}$ events and 24 signal candidate events are observed in data.

Fig. 5 shows the comparison of the Δ distributions in data and MC (NDF, SD and IDP). Good agreement is observed between data and MC except at high values of Δ where EDP dominates. The significance of the excess with respect to the NDF, SD and IDP backgrounds is determined using a modified frequentist method [17]. It is obtained via fits of the signal + background and background-only hypotheses to pseudo-data samples containing only background. The effect of systematic uncertainties is constrained by maximizing a likelihood function for background and signal + background hypotheses over all systematic uncertainties. Pseudo experiments used to determine the significance of the EDP signal include variations over each systematic uncertainty. The observed significance corresponds to the fraction of outcomes that yield an EDP cross section at least as large as that measured in data. Four bins are used as input for the significance calculation: 3 bins for Δ between 0.2 and 0.8, where the predominant region used in the MC normalization is removed, and the $\Delta > 0.8$ bin. The probability for the observed excess to be explained by an upward fluctuation of the background is 2×10^{-6}, corresponding to an excess of 4.7 standard deviations. The expected significance for the EDP signal is estimated to correspond to 4.8 standard deviations. Table 1 gives the observed number of events compared to background and EDP expectations. Fig. 6 displays the dijet invariant mass distribution for $\Delta > 0.8$ without any cut on M_{jj}. Most of the observed events are concentrated at M_{jj} below 160 GeV, where the EDP contribution is expected to be largely dominant, as shown in the Fig. 6. To illustrate the differences between the diffractive dijet exclusive events with $\Delta > 0.8$, where the calorimeter has little energy deposition outside the central region, and the non-diffractive events, two event displays are shown in Fig. 7. The excess in data can contain events where the proton is dissociated into low-mass states that escape detection. The contribution of such events is estimated to be up to 10% of the EDP cross section [9]. The choice of dijet mass requirement was studied and $M_{jj} < 160$ GeV was chosen since it optimizes the expected sensitivity.

To summarize, we have presented evidence at the 4.7 standard deviation level for events consistent with the exclusive dijet production event topology in $p\bar{p}$ collisions at a center-of-mass energy $\sqrt{s} = 1.96$ TeV at high dijet invariant mass ($M_{jj} > 100$ GeV). These are the highest mass states studied for exclusive production in hadron colliders. Such event signatures are expected to play an important role in future studies at the Tevatron and LHC.

Table 1
Number of predicted events for each MC sample for all Δ and for $\Delta > 0.8$ after the selection requirements including $M_{jj} < 160$ GeV. The total uncertainties are quoted.

Sample	NDF	IDP	SD	EDP	Background	Data
All Δ	243 145	52.2	1484.9	49	244 682	244 682
$\Delta > 0.8$	$1.4^{+1.0}_{-0.8}$	$2.2^{+1.8}_{-1.5}$	$0.05^{+0.04}_{-0.03}$	$20.4^{+1.8}_{-1.7}$	$3.7^{+2.4}_{-1.7}$	24

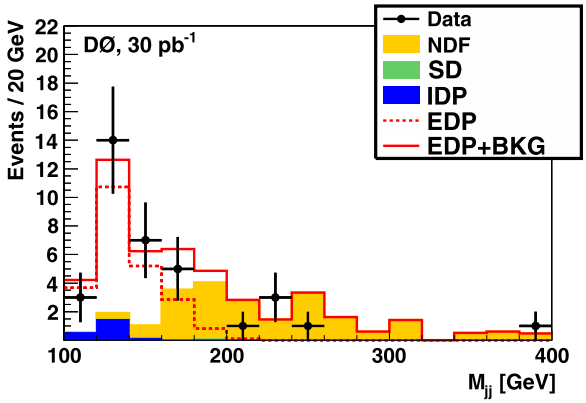

Fig. 6. Dijet invariant mass distribution for data (points) and sum of EDP, NDF, SD and IDP. Separate histograms for signal and background contributions are shown as well. All distributions are for the events with $\Delta > 0.8$.

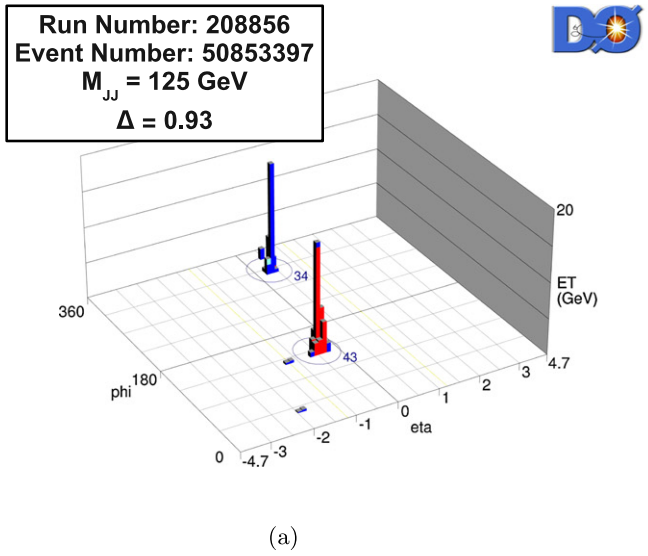

(a)

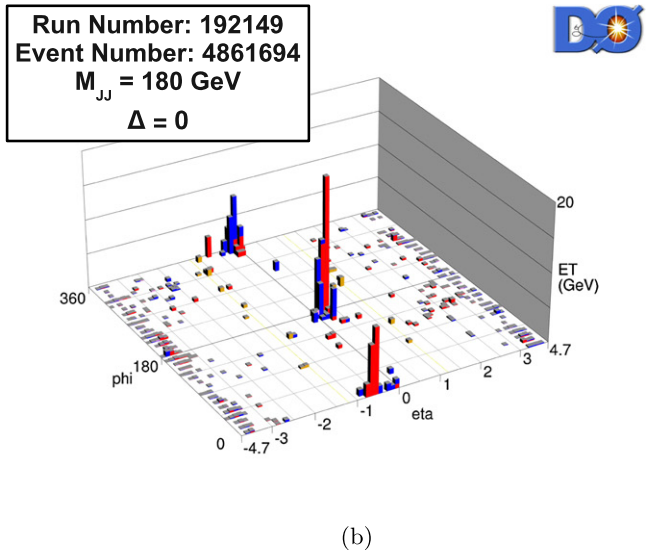

(b)

Fig. 7. Event displays showing E_T in the η–φ plane: (a) Exclusive diffractive event candidate: No energy deposition is present in the forward regions, only two central jets are observed in the detector. (b) Background event: In addition to the two jets present in the detector, energy deposition is present in the forward regions. The different colors correspond to energy deposits in different layers of the calorimeter.

Acknowledgements

We thank the staffs at Fermilab and collaborating institutions, and acknowledge support from the DOE and NSF (USA); CEA and CNRS/IN2P3 (France); FASI, Rosatom and RFBR (Russia); CNPq, FAPERJ, FAPESP and FUNDUNESP (Brazil); DAE and DST (India); Colciencias (Colombia); CONACyT (Mexico); KRF and KOSEF (Korea); CONICET and UBACyT (Argentina); FOM (The Netherlands); STFC and the Royal Society (United Kingdom); MSMT and GACR (Czech Republic); CRC Program and NSERC (Canada); BMBF and DFG (Germany); SFI (Ireland); The Swedish Research Council (Sweden); and CAS and CNSF (China).

References

[1] UA8 Collaboration, R. Bonino, et al., Phys. Lett. B 211 (1988) 239.
[2] H1 Collaboration, A. Aktas, et al., Eur. Phys. J. C 48 (2006) 715;
ZEUS Collaboration, S. Chekanov, et al., Nucl. Phys. B 831 (2010) 1;
ZEUS Collaboration, S. Chekanov, et al., Nucl. Phys. B 713 (2005) 3.
[3] D0 Collaboration, B. Abbott, et al., Phys. Lett. B 531 (2002) 52;
D0 Collaboration, B. Abbott, et al., Phys. Lett. B 574 (2003) 169;
CDF Collaboration, D.E. Acosta, et al., Phys. Rev. Lett. 91 (2003) 011802;
CDF Collaboration, D.E. Acosta, et al., Phys. Rev. Lett. 93 (2004) 141601.
[4] G. Ingelman, P.E. Schlein, Phys. Lett. B 152 (1985) 256;
M. Boonekamp, et al., Acta Phys. Polon. B 40 (2009) 2239, and references therein.
[5] A. Schafer, O. Nachtmann, R. Schopf, Phys. Lett. B 249 (1990) 331;
J.D. Bjorken, Phys. Rev. D 47 (1993) 101.
[6] V.A. Khoze, A.D. Martin, M.G. Ryskin, Eur. Phys. J. C 14 (2000) 525;
V.A. Khoze, A.D. Martin, M.G. Ryskin, Eur. Phys. J. C 19 (2001) 477;
V.A. Khoze, A.D. Martin, M.G. Ryskin, Eur. Phys. J. C 20 (2001) 599, Erratum.
[7] M. Boonekamp, R.B. Peschanski, C. Royon, Phys. Lett. B 598 (2004) 243.
[8] CDF Collaboration, T. Aaltonen, et al., Phys. Rev. D 77 (2008) 052004;
CDF Collaboration, T. Aaltonen, et al., Phys. Rev. Lett. 99 (2007) 242002;
CDF Collaboration, T. Aaltonen, et al., Phys. Rev. Lett. 102 (2009) 222002;
CDF Collaboration, T. Aaltonen, et al., Phys. Rev. Lett. 102 (2009) 242001;
CDF Collaboration, A. Abulencia, et al., Phys. Rev. Lett. 98 (2007) 112001.
[9] J. Monk, A. Pilkington, Comput. Phys. Commun. 175 (2006) 232;
M. Boonekamp, et al., in: Proceedings of the Workshop of the Implications of HERA for LHC Physics, DESY-Proc-2009-02.
[10] H1 Collaboration, A. Aktas, et al., Eur. Phys. J. C 48 (2006) 715.
[11] M.G. Ryskin, A.D. Martin, V.A. Khoze, Eur. Phys. J. C 60 (2009) 265;
E. Gotsman, et al., arXiv:hep-ph/0511060.
[12] T. Sjöstrand, et al., Comput. Phys. Commun. 135 (2001) 238.
[13] B.E. Cox, J.R. Forshaw, Comput. Phys. Commun. 144 (2002) 104.
[14] D0 Collaboration, V.M. Abazov, et al., Nucl. Instrum. Methods Phys. Res. A 565 (2006) 463.
[15] G.C. Blazey, et al., in: U. Baur, R.K. Ellis, D. Zeppenfeld (Eds.), Proceedings of the Workshop: QCD and Weak Boson Physics in Run II, Fermilab-Pub-00/297, 2000.
[16] R. Brun, F. Carminati, CERN Program Library Long Writeup W5013, 1993 (unpublished).
[17] W. Fisher, FERMILAB-TM-2386-E, 2006.